Polymer Chemistry

Accepted Manuscript

This is an *Accepted Manuscript*, which has been through the Royal Society of Chemistry peer review process and has been accepted for publication.

Accepted Manuscripts are published online shortly after acceptance, before technical editing, formatting and proof reading. Using this free service, authors can make their results available to the community, in citable form, before we publish the edited article. We will replace this *Accepted Manuscript* with the edited and formatted *Advance Article* as soon as it is available.

You can find more information about *Accepted Manuscripts* in the Information for Authors.

Please note that technical editing may introduce minor changes to the text and/or graphics, which may alter content. The journal's standard Terms & Conditions and the Ethical guidelines still apply. In no event shall the Royal Society of Chemistry be held responsible for any errors or omissions in this *Accepted Manuscript* or any consequences arising from the use of any information it contains.

ROYAL SOCIETY OF CHEMISTRY

www.rsc.org/polymers

ARTICLE TYPE www.rsc.org/xxxxxx | XXXXXXXX

Unexpected Fluorescence from Maleimide-Containing Polyhedral Oligomeric Silsesquioxanes Nanoparticle and Sequence Distribution Analyses of Polystyrene-Based Alternating Copolymers

Mohamed Gamal Mohamed, Kuo-Chih Hsu, Jin-Long Hong and Shiao-Wei Kuo*

Received (in XXX, XXX) Xth XXXXXXXXX 200X, Accepted Xth XXXXXXXXX 200X
First published on the web Xth XXXXXXXXX 200X
DOI: 10.1039/b000000x

In this study, we synthesized unusual fluorescent polyhedral oligomeric silsesquioxane (POSS)-containing polymers lacking any common fluorescent units (e.g., phenyl or heterocyclic rings): a poly(maleimide isobutyl POSS) [poly(MIPOSS)] homopolymer and poly(styrene-*alt*-maleimide isobutyl POSS) [poly(S-*alt*-MIPOSS] and poly(4-acetoxystyrene-*alt*-malemide isobutyl POSS) [poly(AS-*alt*-MIPOSS)] alternating copolymers, through free radical polymerization, and a poly(4-hydroxystyrene-*alt*-malemide isobutyl POSS) [poly(HS-*alt*-MIPOSS)] alternating copolymer, through acetoxy hydrazinolysis of poly(AS-*alt*-MIPOSS). We used ^{1}H, ^{13}C, and ^{29}Si nuclear magnetic resonance spectroscopy, Fourier transform infrared (FTIR) spectroscopy, and MALDI-TOF mass spectrometry to examine the chemical structures and sequence distributions of these POSS-containing polymers. The FTIR spectra revealed the existence of specific intermolecular interactions, namely dipole-dipole interactions between the C=O groups in poly(MIPOSS) and poly(AS-*alt*-MIPOSS) and intermolecular hydrogen bonding between the C=O groups of the MIPOSS units and the OH groups of the HS units in poly(HS-*alt*-MIPOSS). Differential scanning calorimetry and thermogravimetric analyses revealed that the incorporation of MIPOSS units could enhance the thermal stability, but decrease the glass transition temperatures, of these alternating copolymers. The photoluminescence emission of poly(MIPOSS) was greater than those of the POSS-containing alternating copolymers, presumably because of the former's crystallinity and clustering of locked C=O groups of POSS units.

Introduction

Luminescent materials are attractive for academic research and have technical significance because of their possible applications in drug delivery,[1] chemical sensors,[2] DNA probing,[3] protein sensors,[4] and cellular bioimaging.[5] The most luminescent materials are often quantum dots,[6] fluorescent organic dyes,[7] and fluorescent proteins.[8] Many fluorescent organic materials containing heterocyclic or benzene units exhibit aggregation-caused quenching (ACQ). Such ACQ luminescent materials are highly emissive in solution, but nonemissive in their aggregated or condensed states.[9-11] Tang et al. discovered, however, some small organic and polymeric fluorescent materials, based on silole derivatives, that display strong emissions when concentrated in solution or in the solid state; these materials are aggregation-induced emission (AIE) fluorescent materials.[12-14]

Most fluorescent polymeric materials feature π-aromatic units (benzene or heterocyclic rings) as emissive units.[15,16] Recently, fluorescent polymers lacking such conventional fluorescent units have attracted much attention for their excellent biocompatibility and biodegradability. For example, Tang et al. also found that polymerization of nonluminescent monomers-through free radical polymerization, reversible addition/fragmentation chain transfer (RAFT), or atom transfer radical polymerization-lacking luminescent groups can also give highly emissive polymeric materials.[15,16] In addition, Tang and coworkers observed that alternating poly(vinyl acetate-*alt*-maleic anhydride) nanoparticles exhibited strong light emission and AIE effects because of intermolecular interactions between their five membered dihydrofuran-2,5-dione groups or clustering of their locked C=O groups.[16] In addition, hyperbranched polymers featuring tertiary amino units, including polyureas,[17] poly(ether amide)s,[18] poly(amido amine)s,[19] and poly(amino ester)s,[20] can act as luminescent polymers. The emission mechanism of these materials originates from the presence of the tertiary amino moieties.[21,22] Succinimide derivatives are known fluorescence quenchers of proteins, and maleic anhydride-containing polymers can display fluorescence.[23] Polyisobutene succinic anhydrides and their imides have displayed unexpected emissions that have been attributed to the AIE effects of their C=O groups.[24]

Polyhedral oligomeric silsesquioxane (POSS) and its derivatives comprise an intriguing class of compounds that can be considered as nanostructured inorganic composites or organic/inorganic hybrid materials.[25-30] POSS derivatives have been studied in academic and industrial fields because of their interesting interfacial interactions; they have well-defined cubic three-dimensional cage-like structures with a chemical formula $(RSiO_{1.5})_8$, where the R unit is an organic group that can impart solubility and compatibility within a polymer matrix-indeed, the introduction of POSS moieties into polymer matrices can result in novel polymers displaying interesting mechanical properties, high thermal stabilities, and low flammability.[31–35] Hayakawa and Gopalan successfully synthesized the polystyrene-*b*-PMAPOSS (poly(methacrylate POSS) diblock copolymers with well-defined molecular distributions and high degrees of polymerization; these polymers exhibited microphase-separated structures.[36-38] Monticelli et al. grafted a titanium-containing POSS (M-POSS) to the maleic anhydride groups of a poly(styrene-*alt*-maleic anhydride) copolymer; the resulting nanofiber/M-POSS system displayed good photocatalytic activity for the degradation of sulforhodamino B, an organic dye.[39] Recently, Zhang et al. synthesized the alternating copolymer poly(styrene-*alt*-maleimide isobutyl POSS) [poly(S-*alt*-MIPOSS)] through RAFT polymerization, finding that incorporation of the MIPOSS moieties greatly enhanced the thermal properties of the copolymers.[40] Zhang et al. also demonstrated that poly[MIPOSS-*alt*-vinylbenzyl poly(ethylene glycol)] [poly(MIPOSS-*alt*-

Department of Materials and Optoelectronic Science, Center for Nanoscience and Nanotechnology, National Sun Yat-Sen University, Kaohsiung, 804, Taiwan.
E-mail: kuosw@faculty.nsysu.edu.tw

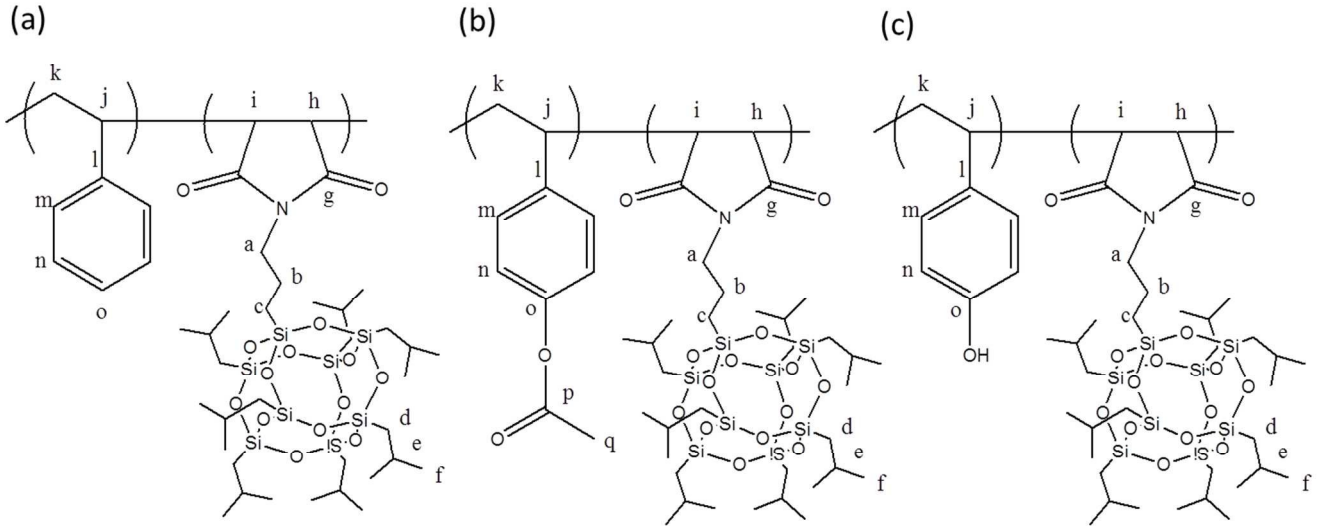

Scheme 1: Chemical Structures and peak assignments for NMR spectra of poly(S-*alt*-MIPOSS), poly(AS-*alt*-MIPOSS) and poly(HS-*alt*-MIPOSS) copolymers

Table 1: Presents the molecule weight, glass transition temperature and quantum yield of poly(MIPOSS), poly(S-alt-MIPOSS), poly(AS-alt-MIPOSS) and poly(HS-alt-MIPOSS)

Sample	M_n[a]	PDI[a]	M_n[b]	PDI[b]	T_g[c] (^oC)	λ_{ab}[d] (nm)	Quantum yield[e] (%)
MIPOSS	2544.1	1.08	2110	1.33	-	237.3/280.0	72.5
S-alt-MIPOSS	3887.9	1.12	14600	1.98	103	236.0/259.3	55.5
AS-alt-MIPOSS	2915.4	1.16	6570	1.64	75	235.7/262.5	46.8
HS-alt-MIPOSS	3155.9	1.16	5370	1.88	96	236.1/278.7	7.0

[a]: Measured by MALDI-TOF MS analysis.
[b]: Measured by GPC.
[c]: Measured by DSC.
[d]: Determined by UV-vis absorption measurement.
[e]: Determined by integrated sphere by ocean optics.

VBPEG)] could self-assemble in aqueous solution to form spherical structures.[41]

In this study, we synthesized a poly(MIPOSS) homopolymer and POSS-containing poly(S-*alt*-MIPOSS) and poly(AS-*alt*-MIPOSS) alternating copolymers through facile and ordinary free radical polymerizations in the presence of AIBN as the initiator in THF solution. We then prepared a poly(HS-*alt*-MIPOSS) alternating copolymer through acetoxy hydrazinolysis of poly(AS-*alt*-MIPOSS) using hydrazine monohydrate in 1,4-dioxane (**Scheme 1**). ^1H, ^{13}C, and ^{29}Si NMR spectroscopy, MALDI TOF mass spectrometry, and Fourier transform infrared (FTIR) spectroscopy confirmed their chemical structures. Furthermore, we employed differential scanning calorimetry (DSC) and thermogravimetric analysis (TGA) to determine the thermal degradation temperatures, char yields, and glass transition temperatures of the POSS-containing homopolymer and the alternating copolymers. FTIR spectra revealed the existence of specific intermolecular interaction, including dipole-dipole and hydrogen bonding interactions, in these POSS-containing polymers. We used wide-angle X-ray diffraction (WAXD) to examine the crystallinity of these POSS-containing polymers, and photoluminescence (PL) spectroscopy to study the optical properties of our POSS-containing alternating copolymers in solution and in the bulk state. To the best of our knowledge, we are first to report the unusual fluorescent polyhedral oligomeric silsesquioxane (POSS)-containing polymers (poly(maleimide isobutyl POSS) lacking any common fluorescent unit by simple free radical polymerization and study their emission behavior in solid and solution states. In addition, we expect that these fluorescent alternating polymeric materials containing POSS nanoparticles can result in dramatic improvements in the physical properties such as reduction in flammability and oxidation resistance.

Experimental Section

Materials

Maleimide isobutyl POSS (MIPOSS) was purchased from Hybrid Plastics Company and used without purification. Methanol (MeOH), dichloromethane (DCM), tetrahydrofuran (THF), and hydrazine monohydrate ($N_2H_4{\cdot}H_2O$) were purchased from Alfa-Aesar. Azobisisobutyronitrile (AIBN) was received from Sigma-Aldrich, recrystallized (MeOH) three times, and stored in a refrigerator to avoid decomposition. Styrene and 4-acetoxystyrene were purchased from Sigma-Aldrich; prior to polymerization, they were passed through an aluminum oxide column to remove any inhibitor and dried over CaH_2 for 24 h under a N_2 atmosphere. Polystyrene (molecular weight: 35000 g/mol) was purchased from Sigma-Aldrich; poly(styrene-*alt*-maleic anhydride) (S-*alt*-MA) was synthesized according to a previous report.[16]

MIPOSS Homopolymer through Free Radical Polymerization

MIPOSS (3.00 g, 3.15 mmol) and AIBN (0.150 g) were dissolved in dry THF (30 mL) under a N_2 atmosphere in a 50-mL two-necked round-bottom flask equipped with a stirrer bar. The solution was carefully degassed through three freeze/thaw cycles

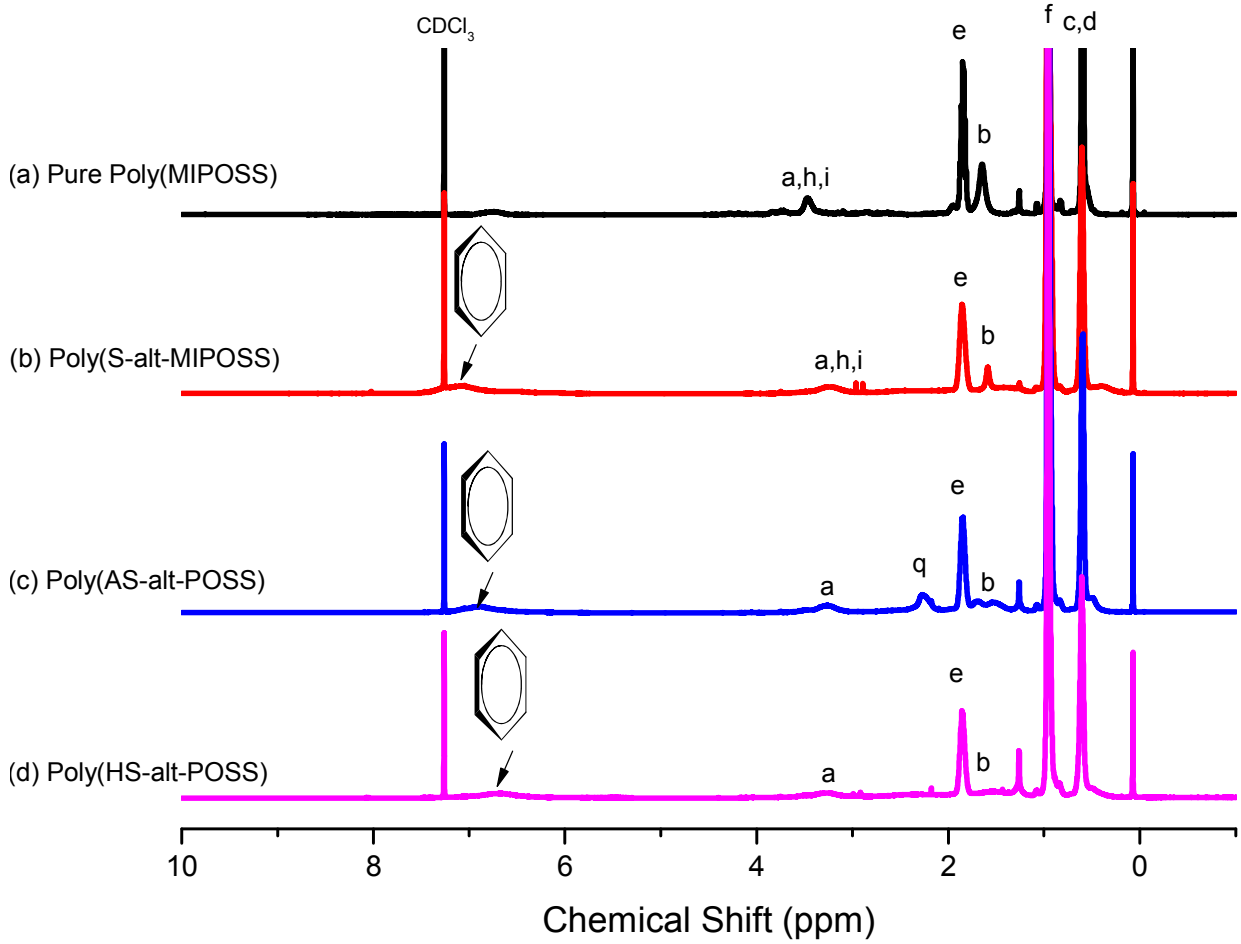

Figure 1: ^{1}H NMR spectra of (a) poly(MIPOSS), (b) poly(S-*alt*-MIPOSS), (c) poly(AS-*alt*-MIPOSS), and (d) poly(HS-*alt*-MIPOSS) in $CDCl_3$.

to remove any O_2. The mixture was then heated at 70-80 °C for 24 h. The polymerization was quenched by cooling the flask in an ice bath and exposing the contents to air for 1 h. The crude polymer was precipitated from the reaction mixture into a large amount of cold MeOH. This crude polymer was then reprecipitated from cold THF/MeOH three times to remove any unreacted MIPOSS monomer and other byproducts. The resulting homopolymer was dried at 50 °C for 24 h under high vacuum to remove any residual solvents. ^{1}H NMR (500 MHz, $CDCl_3$, δ, ppm): 3.41 (polymer backbone and NC**H**$_2$CH$_2$), 1.85 [C**H**$(CH_3)_2$], 1.60 (SiC**H**$_2$CH$_2$), 0.96 [CH(C**H**$_3)_2$], 0.603 (SiC**H**$_2$). ^{13}C NMR (125 MHz, $CDCl_3$, δ, ppm): 177.58 (maleimide C=O), 41.62, 32.21, 29.34, 26.07, 25.73, 21.39, 9.45. FTIR (KBr, cm^{-1}): 1777 (asymmetric imide C=O stretching), 1709 (symmetric imide C=O stretching), 2946-2887 (isobutyl CH stretch), 1227 (CN bending vibration), and 1110 (Si-O-Si stretching of POSS core).

Poly(S*-alt-*MIPOSS) and Poly(AS*-alt-*MIPOSS) Alternating Copolymers

MIPOSS (3.00 g, 3.15 mmol), styrene (0.328 g, 3.15 mmol) or 4-acetoxystyrene (0.511 g, 3.15 mmol), and AIBN (5 wt%) were dissolved in dry THF (50 mL) under a N_2 atmosphere in a 100-mL two-necked round-bottom flask equipped with a stirrer bar. The solution was carefully degassed through three freeze/thaw cycles to remove any O_2 and then heated at 70-80 °C for 24 h. The polymerization was quenched through cooling the flask in an ice bath and exposing the contents to air for 1 h. The crude polymer was obtained through precipitation of the reaction solution into a large amount of cold MeOH. For crude polymer was the reprecipitated from cold THF/MeOH many times to remove any unreacted MIPOSS, styrene or acetoxystyrene, and others impurities. The resulting alternating copolymer was dried at 50 °C for 24 h under high vacuum to remove any residual solvent. For poly(S-*alt*-MIPOSS): ^{1}H NMR (500 MHz, $CDCl_3$, δ, ppm): 7.05 (ArH in polystyrene backbone), 3.41 (polymer backbone and NC**H**$_2$CH$_2$), 1.85 [C**H**$(CH_3)_2$], 1.60 (SiC**H**$_2$CH$_2$), 0.96 [CH(C**H**$_3)_2$], 0.60 (SiC**H**$_2$). ^{13}C NMR (125 MHz, $CDCl_3$, δ, ppm): 178.31 (maleimide C=O), 169.63, 151.21, 130.58, 122.64, 41.62, 30.07, 9.84. FTIR (KBr, cm^{-1}): 1772 (asymmetric C=O stretching, imide and C=O, $OCOCH_3$ group), 1705 (symmetric imide C=O stretching), 1227 (CN bending), 1110 (Si-O-Si stretching of POSS core). For poly(AS-*alt*-MIPOSS), most of the signals in the ^{1}H and ^{13}C NMR spectra were the same as those for poly(S-*alt*-MIPOSS), with the following exceptions: ^{1}H NMR, 2.27 ($OCOCH_3$); ^{13}C NMR, 179.07 (C=O imide), 170.05 (C=O acetate), 21.40 (CH_3).

Poly(HS*-alt-*MIPOSS) Alternating Copolymer

A solution of poly(AS-*alt*-MIPOSS) (2.00 g) in 1,4-dioxane (25 mL), in a 50-mL two-necked round-bottom flask equipped with a stirrer bar, was placed in an ice bath at 0 °C for 30 min under a N_2 atmosphere and then hydrazine monohydrate (15.5 g, 3.10 mmol) was added dropwise. The reaction mixture was then stirred overnight at room temperature. The organic phase was

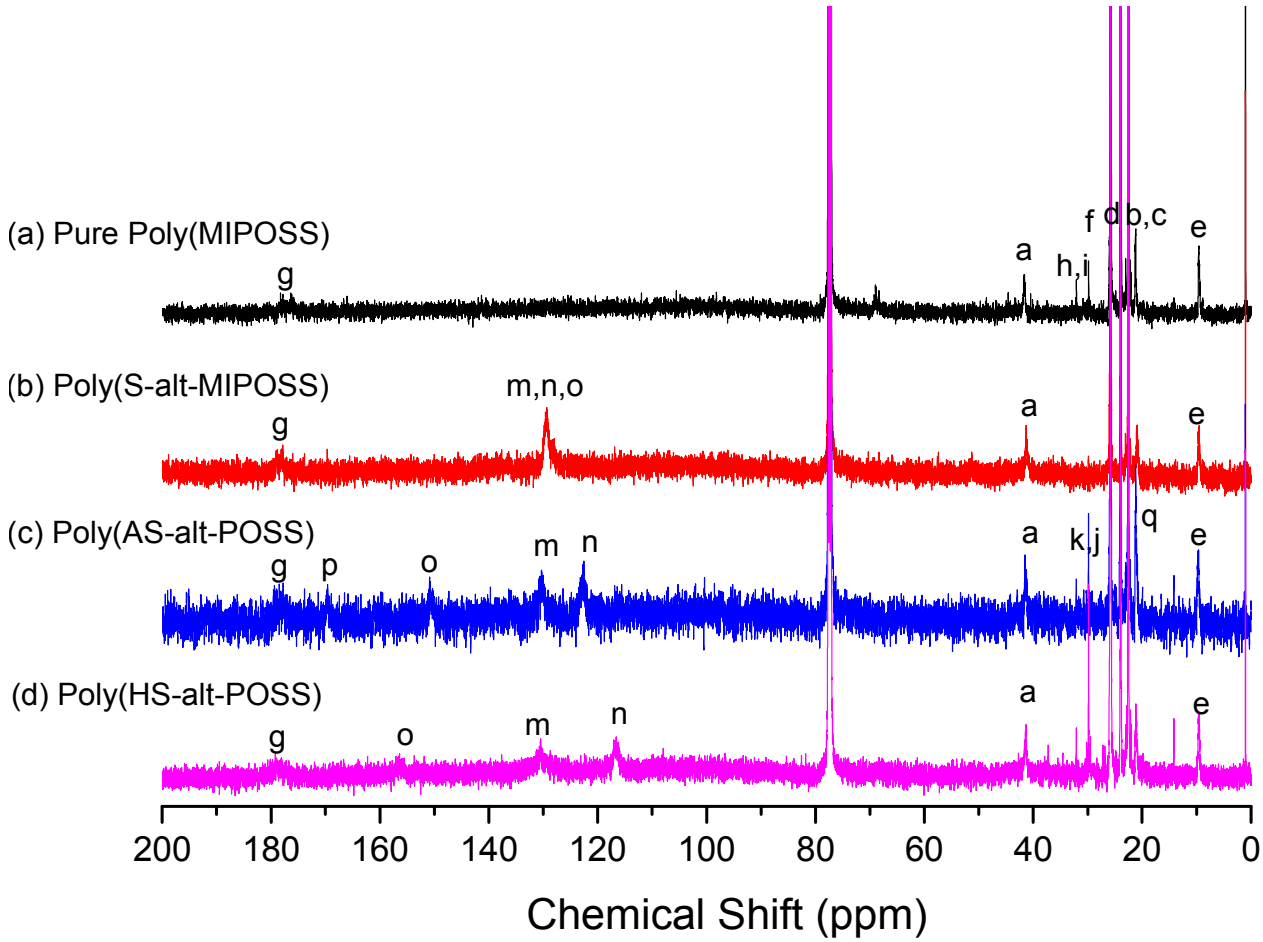

Figure 2: ^{13}C NMR spectra of (a) poly(MIPOSS), (b) poly(S-*alt*-MIPOSS), (c) poly(AS-*alt*-MIPOSS), and (d) poly(HS-*alt*-MIPOSS) in $CDCl_3$.

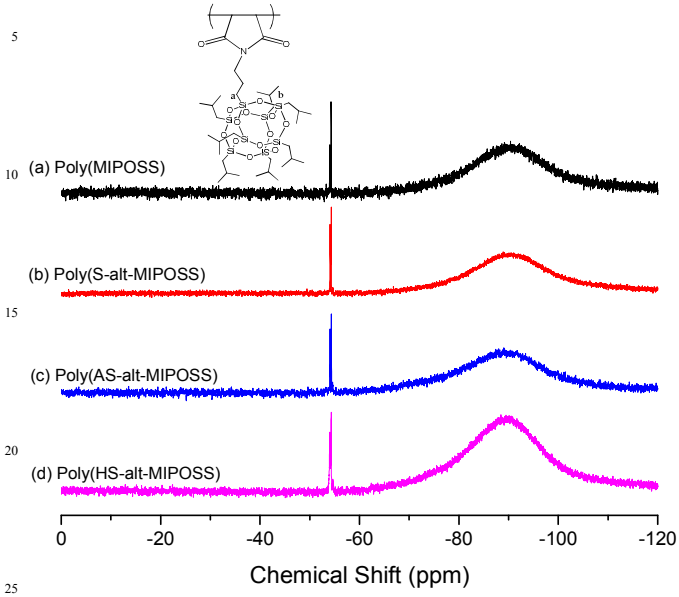

Figure 3: ^{29}Si NMR spectra of (a) poly(MIPOSS), (b) poly(S-*alt*-MIPOSS), (c) poly(AS-*alt*-MIPOSS), and (d) poly(HS-*alt*-MIPOSS) in $CDCl_3$.

extracted into DCM (3 × 50 mL) to remove any excess hydrazine monohydrate. The combined organic phases were dried ($MgSO_4$) for 1 h and then removed DCM solution by rotary evaporator to give a white powder. ^{1}H NMR (500 MHz, $CDCl_3$, δ, ppm): 7.05 (ArH in polystyrene backbone), 3.23 (polymer backbone and N**C**$H_2$$CH_2$), 1.83 [**CH**$(CH_3)_2$], 1.65 (N$CH_2$**C**$H_2$). ^{13}C NMR (125 MHz, $CDCl_3$, δ, ppm): 179.42 (maleimide C=O), 156.62, 130.58, 116.49, 41.62, 29.34, 9.84. FTIR (KBr, cm^{-1}): 3390 (OH stretching), 2946-2887 (isobutyl group), 1774 (asymmetric C=O, imide), 1704 (symmetric C=O stretching, imide), 1227 (CN bending), 1110 (Si-O-Si stretching of POSS core). Table 1 summarizes the properties of poly(MIPOSS) homopolymer and these three alternating copolymers.

Characterization

^{1}H and ^{13}C NMR spectra were recorded using an INOVA 500 with $CDCl_3$ as the solvent with tetramethylsilane (TMS) as an internal reference. FTIR spectra of polymer films were measured using a Bruker Tensor 27 FTIR spectrophotometer; 32 scans were collected at a spectral resolution of 4 cm^{-1}. Mass spectra were recorded using a Bruker Daltonics Autoflex III MALDI-TOF mass spectrometer and the following voltage parameters: 19.06 and 16.61 kV for ion sources; 8.78 kV for lens; and 21.08 and 9.73 kV for reflectors. DSC measurements were preformed using a TA Q-20 system, under N_2 as a purge gas (50 mL/min), and at a heating rate of 20 °C/min. The sample (ca. 3-5 mg) was placed in a sealed aluminum sample pan. The thermal stabilities of the homopolymer and alternating copolymers were investigated using a TA Q-50 thermogravimetric analyzer, under N_2 as a purge gas (60 mL/min), and at a heating rate of 20 °C/min from 30 to 800

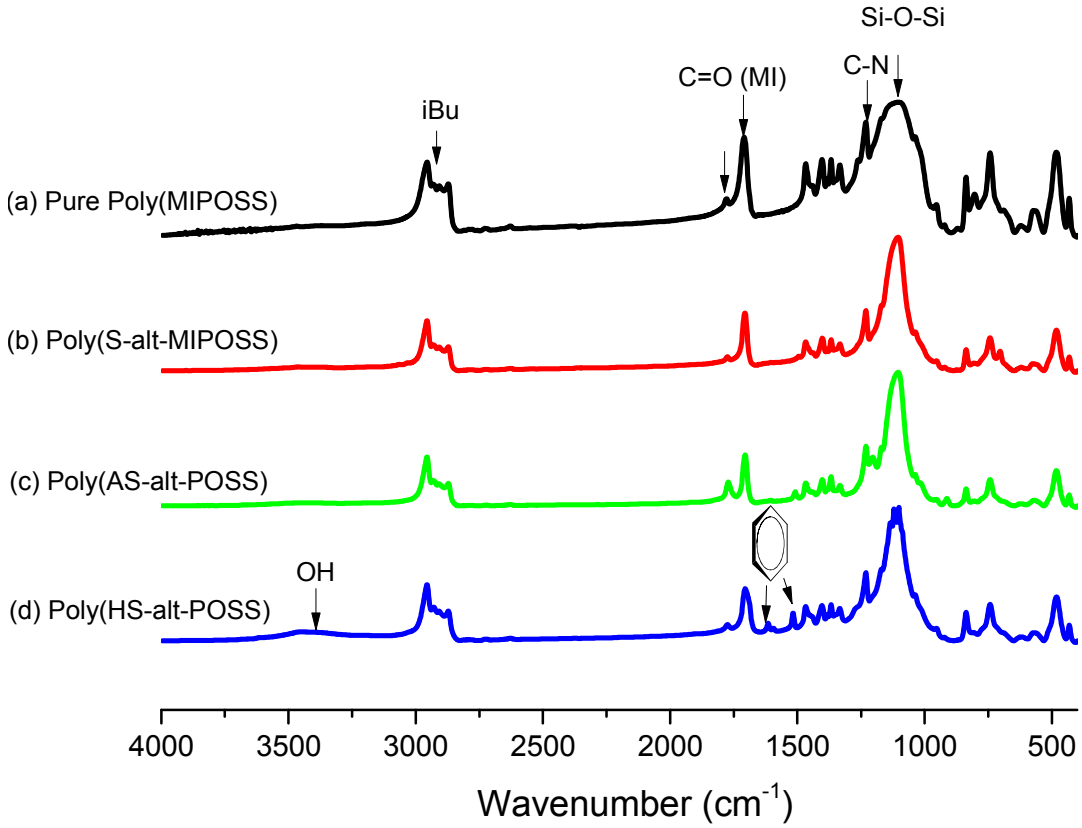

Figure 4: FTIR spectra of (a) poly(MIPOSS), (b) poly(S-*alt*-MIPOSS), (c) poly(AS-*alt*-MIPOSS), and (d) poly(HS-*alt*-MIPOSS) at room temperature.

°C. Molecular weights and molecular weight distributions (PDI) were determined through gel permeation chromatography (GPC) using a Waters 1515 HPLC equipped with refractive index detector and three ultrastragel columns. The GPC system was calibrated using polystyrene as the standard and THF was used as eluent at a flow rate of 1 mL min^{-1}. UV-Vis spectra were recorded using a Shimadzu mini 1240 spectrophotometer; the concentration of polymers in THF was 10^{-4} M. PL spectra were collected at room temperature using a monochromatized Xe light source, solutions of polymers in THF at a concentration of 10^{-4} M, and an excitation wavelength at 330 nm. WAXD profiles were measured using the wiggler beamline BL17A1 of the National Synchrotron Radiation Research Center (NSRRC) of Taiwan. A triangular bent Si (111) single crystal was used to obtain a monochromated beam with a wavelength (λ) of 1.33 Å. The samples were annealed prior to WAXD measurement. The quantum efficiencies (Φ_f) of poly(MIPOSS), poly(S-*alt*-MIPOSS), poly(AS-*alt*-MIPOSS), poly(HS-*alt*-MIPOSS), and poly(S-*alt*-MA) in the solid state were measured in an integrated sphere (Ocean Optics). The quantum efficiencies (Φ_f) of poly(MIPOSS), poly(S-alt-MIPOSS), poly(AS-alt-MIPOSS), poly(HS-alt-MIPOSS), and poly(S-alt-MA) in the solution state were determined by using a quinine sulfate as the standard solutions. Particles sizes of the shrunken aggregates of poly(MIPOSS) and poly(S-alt-MIPOSS) in THF/H_2O mixed media were evaluated by dynamic light scattering (DLS) using a Brookhaven 90 plus spectrometer equipped with a temperature controller.

Results and Discussion

The incorporation of POSS into a polymer matrix can afford organic/inorganic hybrid materials displaying good thermal stability, oxidation resistance, and high mechanical properties.[26,40,41] In this study, we synthesized four new POSS-containing polymers: a poly(MIPOSS) homopolymer and poly(S-*alt*-MIPOSS) and poly(AS-*alt*-MIPOSS) alternating copolymers, prepared through simple and convenient free radical polymerization using AIBN as the initiator, and a poly(HS-*alt*-MIPOSS) alternating copolymer, prepared through deacetylation of poly(AS-*alt*-MIPOSS) in 1,4-dioxane/hydrazine monohydrate at room temperature. We used ^{1}H, ^{13}C, and ^{29}Si NMR spectroscopy, FTIR spectroscopy, GPC (Figure S1) and MALDI-TOF mass spectrometry to confirm the molecular structures of these POSS-containing polymers. Figure 1 displays the ^{1}H NMR spectra of poly(MIPOSS) and the alternating copolymers. The ^{1}H NMR spectrum of the poly(MIPOSS) homopolymer [Figure 1(a)] features a signal at 3.45 ppm representing the main chain of the maleimide isobutyl POSS; a signal for the $SiCH_2CH_2C\mathbf{H}_2N$ methylene protons at 3.45 ppm; signals at 1.82, 1.65, and 0.94 ppm for the $SiCH_2C\mathbf{H}(CH_3)_2$ methine, $SiCH_2C\mathbf{H}_2CH_2N$ methylene, and $SiCH_2CH(C\mathbf{H}_3)_2$ methyl groups, respectively; and a signal at 0.57 ppm for both the $SiC\mathbf{H}_2CH_2CH_2N$ and $SiC\mathbf{H}_2CH(CH_3)_2$ methylene groups.[40,42] The ^{1}H NMR spectra of poly(S-*alt*-MIPOSS), poly(AS-*alt*-MIPOSS), and poly(HS-*alt*-MIPOSS) [Figures 1(b)-(d), respectively] feature additional signals between 6.67 and 7.06 ppm representing the protons of their aromatic moieties. Moreover, the signal at 2.27 ppm (peak ***q***) in the spectrum of poly(AS-*alt*-MIPOSS) [**Figure 1(c)**], representing the protons of the acetyl groups ($OCOC\mathbf{H}_3$), disappeared completely after hydrolysis to the OH groups of poly(HS-alt-MIPOSS) [**Figure 1(d)**].[42] Scheme 1 summarizes the other peak assignments.

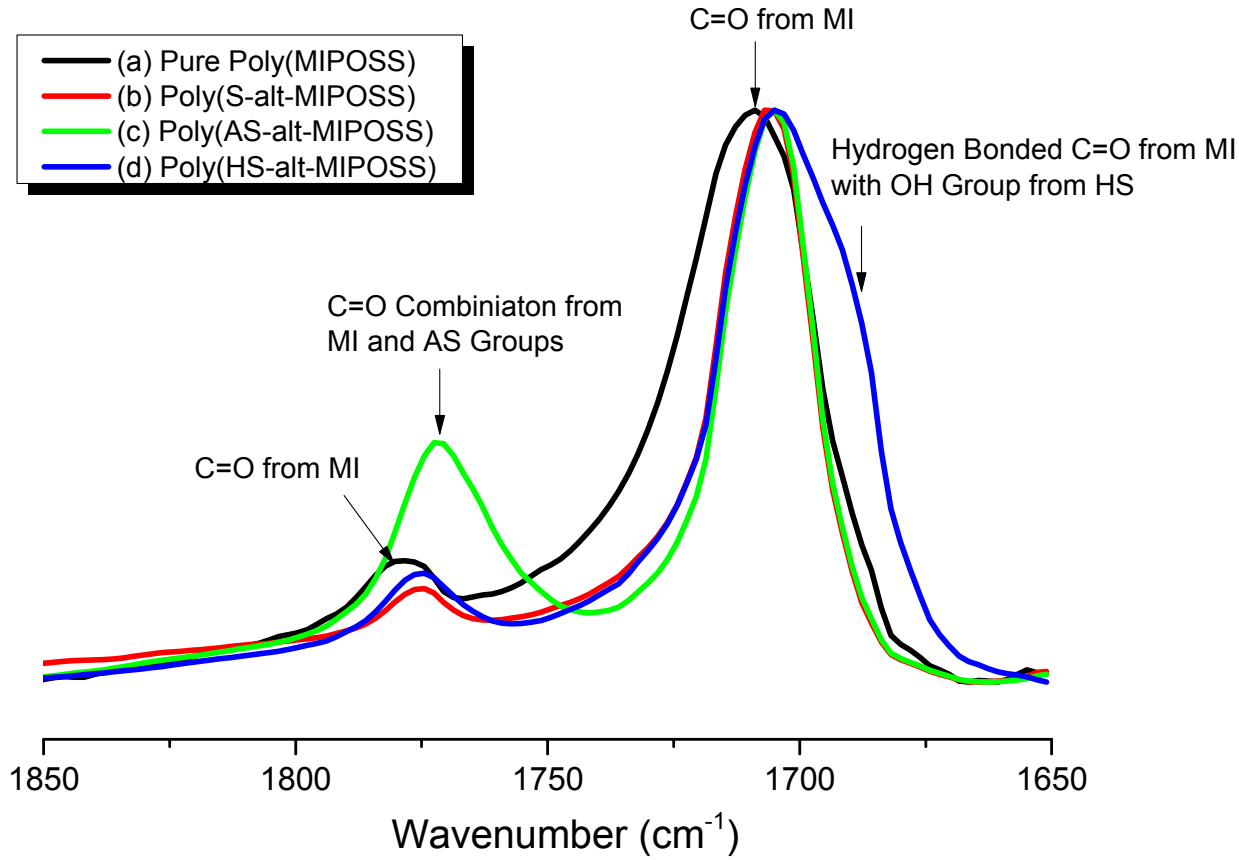

Figure 5: FTIR spectra, in the range 1850–1650 cm^{-1}, of (a) poly(MIPOSS), (b) poly(S-*alt*-MIPOSS), (c) poly(AS-*alt*-MIPOSS), and (d) poly(HS-*alt*-MIPOSS), recorded at room temperature.

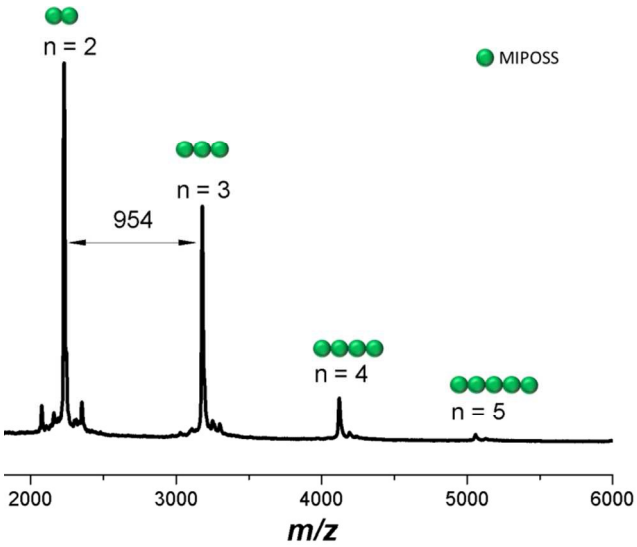

Figure 6: MALDI-TOF mass spectrum of poly(MIPOSS).

Figure 2 displays the ^{13}C NMR spectra of these four polymeric compounds. The ^{13}C NMR spectrum of poly(MIPOSS) in $CDCl_3$ at room temperature [Figure 2(a)] features signals at 177.96, 41.28, and 9.45 ppm, representing the resonances of the carbon nuclei of the **C**=O groups, the $SiCH_2CH_2\mathbf{C}H_2N$ methylene unit, and the $SiCH_2\mathbf{C}H(CH_3)_2$ methine unit, respectively. The spectrum of poly(S-*alt*-MIPOSS) [**Figure 2(b)**] features an additional signal centered at 129.15 ppm, representing the carbon nuclei of the aromatic units. The signals of poly(AS-*alt*-MIPOSS) [Figure 2(c)] appear at 179.07, 170.05, 151.23-123.01, and 21.40 ppm, corresponding to the imide C=O, acetyl C=O, aromatic, and $OCO\mathbf{C}H_3$ methyl groups, respectively. In Figure 2(d), the absence of the signal (170.05 ppm) of the C=O group of the acetate units and the shifts of the signals of the carbon nuclei of the aromatic rings, to 156.09 (**Ph**OH, peak **o**) and 116.66 (peak **n**) ppm, confirmed the synthesis of poly(HS-*alt*-MIPOSS). Scheme 1 summarizes the other peak assignments. We could also use ^{13}C NMR spectroscopy to investigate the alternating copolymers of the maleimide isobutyl POSS and styrene derivatives; the signals of the quaternary carbon nuclei in the aromatic styrene units appear at 151.23–123.01 ppm, indicating that the sequence structures of the copolymers were non-alternating, semi-alternating, and alternating.[40,43,44] **Figure 3** presents the ^{29}Si NMR spectra of poly(MIPOSS), poly(S-*alt*-MIPOSS), poly(AS-*alt*-MIPOSS), and poly(HS-*alt*-MIPOSS) in $CDCl_3$. Two peaks appear, centered at -54.02 (peak **a**) and -54.44 ppm (peak **b**), corresponding to their $O\mathbf{Si}CH_2CH_2CH_2N$ and $O\mathbf{Si}CH_2CH(CH_3)_2$ units, respectively. These ^{29}Si NMR spectra suggest that no cage cleavage occurred during the free radical polymerization, with the POSS cores remaining intact. Taken together, the NMR spectra are consistent with the chemical structures of the homopolymer and alternating copolymers.

Figure 4 displays the FTIR spectra of poly(MIPOSS), poly(S-*alt*-MIPOSS), poly(AS-*alt*-MIPOSS), and poly(HS-*alt*-MIPOSS) at room temperature. Characteristic absorption bands of the homopolymer and alternating copolymers appear at 2952-2874, 1781, 1709, and 1110 cm^{-1}, representing isobutyl CH stretching, asymmetric imide C=O stretching, symmetric imide

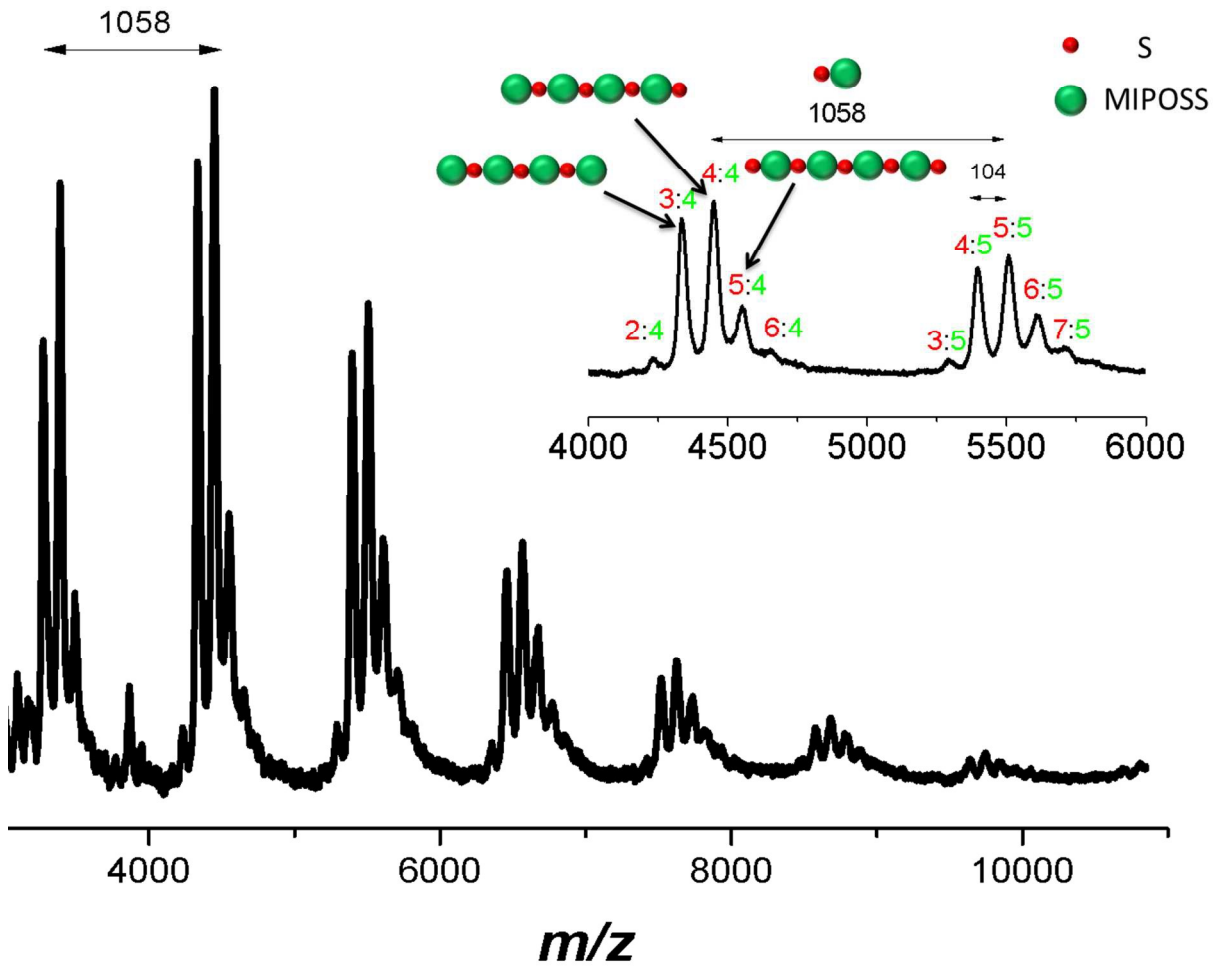

Figure 7: MALDI-TOF mass spectrum of poly(S-*alt*-MIPOSS).

C=O stretching, and Si-O-Si stretching in the maleimide isobutyl POSS structure. The spectrum of poly(HS-*alt*-MIPOSS) [**Figure 4(d)**] features an absorption band at 3453 cm^{-1} for OH stretching; the signal at 1771 cm^{-1} for C=O stretching of the AS groups in Figure 4(c) only decreased after deacetylation because it overlapped with the signal for asymmetric imide C=O stretching.

Figure 5 displays FTIR spectra, in the range 1850-1650 cm^{-1}, that reveal the presence of specific interactions in the alternating polymers. The spectrum of poly(MIPOSS) [**Figure 5(a)**] features two characteristic absorption bands centered at 1781 and 1709 cm^{-1}, corresponding to asymmetric imide C=O and symmetric imide C=O stretching, respectively. These absorption bands shifted to lower frequencies for poly(S-*alt*-MIPOSS) [to 1774 and 1706 cm^{-1}, respectively; Figure 5(b)] and poly(AS-*alt*-MIPOSS) [to 1771 and 1705 cm^{-1}, respectively; Figure 5(c)]. More interestingly, the width at half-height decreased from 32.3 cm^{-1} for poly(MIPOSS) to 19.8 and 20.2 cm^{-1} for poly(S-*alt*-MIPOSS) and poly(AS-*alt*-MIPOSS), respectively, implying that the dipole-dipole interactions between the imide C=O groups of poly(MIPOSS) were disrupted and weakened upon insertion of the styrene and acetoxystyrene segments. The FTIR spectrum of poly(HS-*alt*-MIPOSS) [Figure 4(d)] reveals that the signals of the C=O groups shifted to 1774 and 1704 cm^{-1}, respectively, with a new signal appearing at 1688 cm^{-1}, suggesting that hydrogen bonds existed between the C=O groups of the MIPOSS units and the phenolic OH groups of the HS units.[45] Through curve-fitting with the Gaussian function, we calculated the area fraction of the hydrogen-bonded C=O groups of the MIPOSS units to be 39.3%.

We recorded MALDI-TOF mass spectra to determine the molecular weights of our POSS-containing polymers and the sequence distributions of our alternating copolymers. It can be difficult to measure MALDI-TOF profiles of high-molecular-weight compounds because the mass resolution can be too weak to separate the individual chains.[46-48] **Figure 6** displays the MALDI-TOF mass spectrum of poly(MIPOSS), revealing that the molar mass of its individual chains could be determined. For example, the intense peaks *m*/*z* 2230.80, 3184.95, 4124.30, and 5065.17 correspond to two, three, four, and five units, respectively, of maleimide isobutyl POSS. The difference in the values of *m*/*z* between 2230.95 and 3184.30 is 954, equal to the molecular weight of the repeat unit of poly(MIPOSS). The difference in the values of *m*/*z* between 3184.95 and 4124.30 is not, however, equal to 954, probably because of the different chain ends after thermal fragmentation of AIBN after free radical polymerization.

Figure 7 presents the mass spectrum of poly(S-*alt*-MIPOSS), where the intensities of the individual peaks are not exactly 100%, providing excellent evidence for its copolymer composition: perfectly alternating individual chains with equal numbers of styrene and MIPOSS units. By using MIPOSS as a monomer for free radical copolymerization, it became easy to distinguish the sequence distribution in the MALDI-TOF mass spectrum;

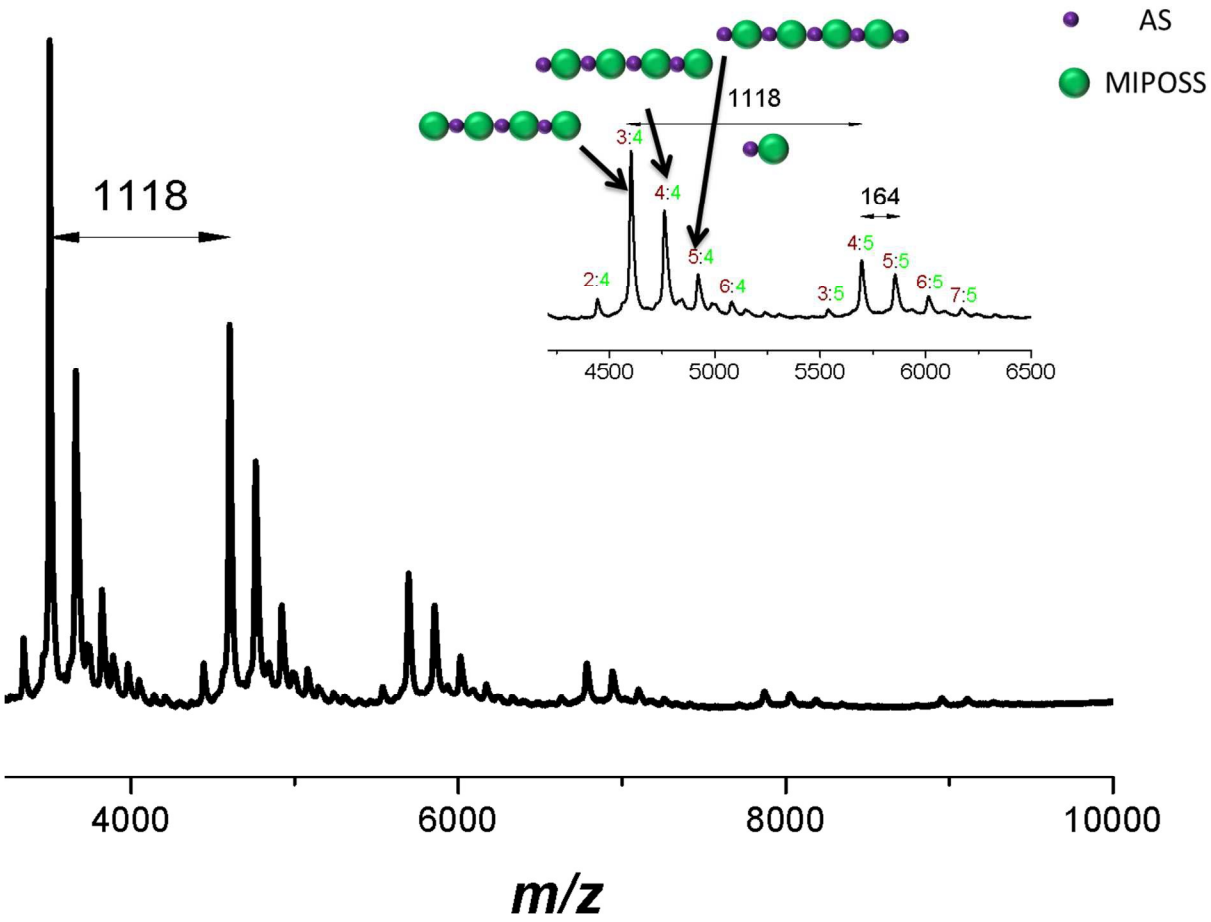

Figure 8: MALDI-TOF mass spectrum of poly(AS-*alt*-MIPOSS).

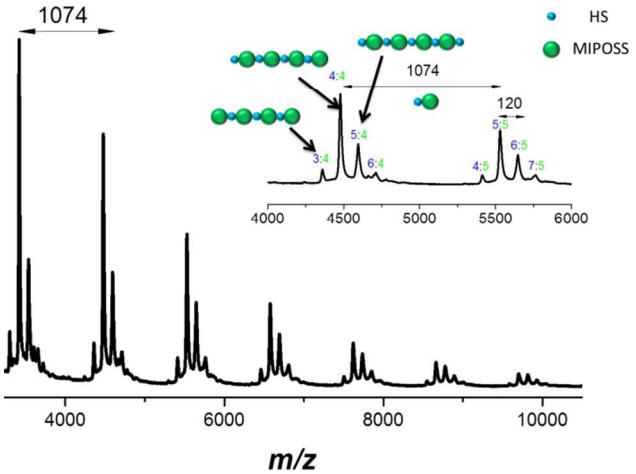

Figure 9: MALDI-TOF mass spectrum of poly(HS-*alt*-MIPOSS).

because the molecular weight of MIPOSS is quite high (954 g/mol), we could readily determine the number of units of MIPOSS in the poly(S-*alt*-MIPOSS) alternating copolymer. For example, the peak at *m*/*z* 4448.72 corresponds to four units of styrene and four units of MIPOSS, while that at *m*/*z* 5506.79 corresponds to five units of styrene and five units of MIPOSS, indicating that poly(S-*alt*-MIPOSS) had a perfectly alternating sequence of individual chains. The difference in the values of *m*/*z* between 4448.72 and 5506.79 is 1058 g/mol, equal to the molecular weight of one styrene and one MIPOSS unit. The intense peak at *m*/*z* 4448.72 corresponds to four units of styrene (4 × 104.15 u), four units of MIPOSS (4 × 954 u), a chain end from AIBN, and a Ag ion (107.87 u); it is labeled 4:4. The most intense peaks correspond to a perfectly alternating sequence, with ratios of styrene:MIPOSS of *n*-1:*n*, *n*:*n*, and *n*+1:*n*, such as 3:4, 4:4, and 5:4 (see inset to Figure 7). Only a few weak peaks correspond to ratios of styrene:MIPOSS of *n*-2:*n* and *n*+2:*n*, such as 2:4 and 6:4, arising due to homopolymerization of styrene and MIPOSS; the fraction of such non-alternating segments was only 3.9%, based on the results of curve-fitting. Thus, MALDI-TOF mass spectral analysis suggested that we had obtained a near-perfect alternating copolymer of poly(S-*alt*-MIPOSS).

Interestingly, the mass spectrum of poly(AS-*alt*-MIPOSS) (**Figure 8**) exhibited the same phenomena as that of poly(S-*alt*-MIPOSS); for example, an intense peak at *m*/*z* 4761.6 (labeled 4:4) corresponding to four units of 4-acetoxystyrene (4 × 162.19 u), four units of MIPOSS (4 × 954 u), a chain end from AIBN, and a Ag ion (107.87 u), as well as a peak at *m*/*z* 5879.3 (labeled 5:5) representing five units of MIPOSS and five units of 4-acetoxystyrene. The difference in the values of *m*/*z* between

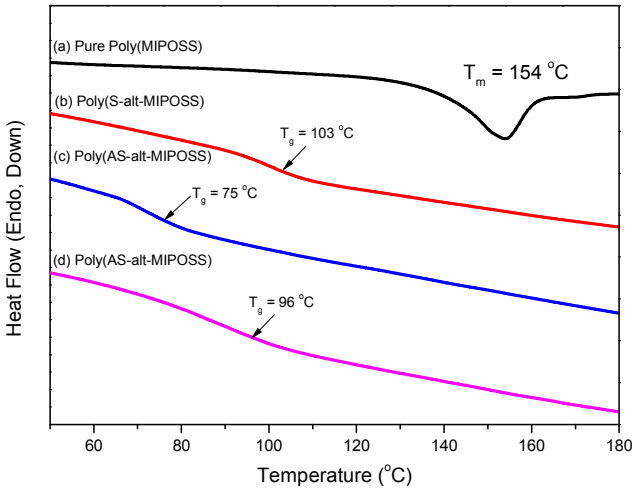

Figure 10: DSC thermograms of (a) poly(MIPOSS), (b) poly(S-*alt*-MIPOSS), (c) poly(AS-*alt*-MIPOSS), and (d) poly(HS-*alt*-MIPOSS).

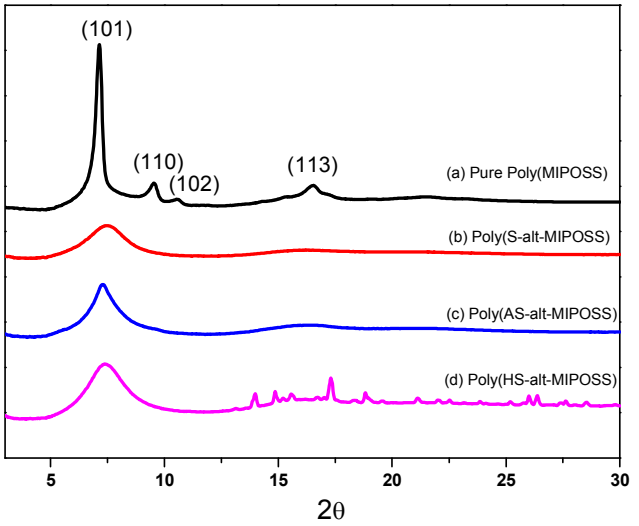

Figure 11: Wide-angle X-ray diffraction (WAXD) patterns of (a) poly(MIPOSS), (b) poly(S-alt-MIPOSS), (c) poly(AS-alt-MIPOSS) and (d) poly(HS-alt-MIPOSS) alternating copolymers.

4761.6 and 5879.3 is 1118 g/mol, equal to the molecular weight of one 4-acetoxystyrene unit and one MIPOSS unit. Similarly, only a few weak peaks appeared corresponding to ratios of 4-acetoxystyrene:MIPOSS of *n*-2:*n* and *n*+2:*n*, such as 2:4 and 6:4, arising from homopolymerization of 4-acetoxystyrene and MIPOSS units, with the fraction of non-alternating segments being only 2.7% based on curve-fitting. This MALDI-TOF mass spectral analysis also implies that we had obtained a near-perfect alternating copolymer of poly(AS-*alt*-MIPOSS). The MALDI-TOF mass spectrum in **Figure 9** confirms that the chain of poly(HS-*alt*-MIPOSS) was also an alternating copolymer, with the intense peak at *m*/*z* 4478.6 (labeled 4:4) representing four units of 4-hydroxystyrene (4 × 120 u), four units of MIPOSS (4 × 954 u), a chain end from AIBN, and a Ag ion (107.87 u), as well as a signal at *m*/*z* 5552.3 (labeled 5:5) attributable to five units of MIPOSS and five units of 4-hydroxystyrene. The difference in the values of *m*/*z* between 4478.6 and 5552.3 is 1074 g/mol, equal to the molecular weight of one 4-hydroxystyrene unit and one

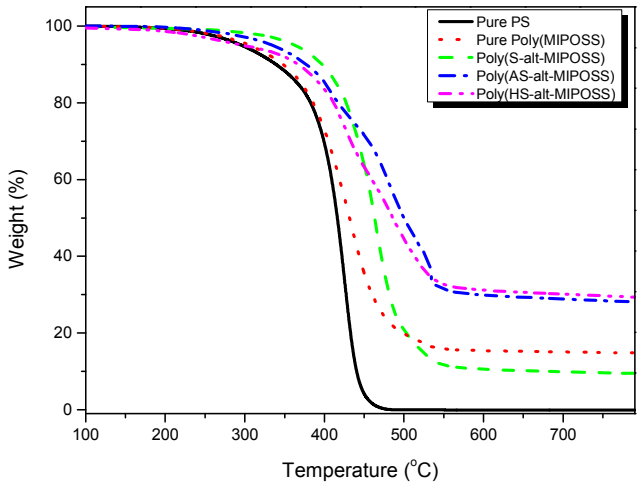

Figure 12: TGA profiles of PS, poly(MIPOSS), poly(S-*alt*-MIPOSS), poly(AS-*alt*-MIPOSS), and poly(HS-*alt*-MIPOSS), recorded under a N_2 atmosphere.

MIPOSS unit. The sequence distribution of poly(HS-*alt*-MIPOSS) should be the same as that of poly(AS-*alt*-MIPOSS), because we prepared it through deacetylation of the latter. Based on their MALDI-TOF mass spectra, our three copolymers appeared to be near-perfect alternating copolymers.

Thermal Properties of Homopolymer and Alternating Copolymers

To elucidate the thermal properties of the homopolymer and alternating copolymers, were subjected them all to DSC and TGA under a N_2 atmosphere. **Figure 10** presents the DSC profiles of poly(MIPOSS), poly(S-*alt*-MIPOSS), poly(AS-*alt*-MIPOSS), and poly(HS-*alt*-MIPOSS). The DSC trace of poly(MIPOSS) [**Figure 10(a)**] features an endothermic melting point at 154 °C and an exothermic crystalline peak at 70 °C (data non shown), suggesting that poly(MIPOSS) possessed a crystalline structure because of POSS aggregation. The introduction of POSS into a polymer can increase the glass transition temperature (T_g) of the resulting organic/inorganic hybrid material because of the rigid structure of the POSS cages and the restricted movement of the polymer chains.[40,42] The glass transition temperature (103 °C) of poly(S-*alt*-MIPOSS) [**Figure 10(b)**] was higher than that of PS at a similar molecular weight (T_g = 90 °C; 5000 g/mol), presumably because of the rigid cage structure of the MIPOSS units. An unusual and interesting phenomenon is evident in **Figures 10(c)** and **10(d)**. The value of T_g of poly(AS-*alt*-MIPOSS) decreased to 75 °C while that of poly(HS-*alt*-MIPOSS) increased to 96 °C after deacetylation, due to hydrogen bonding between the OH groups of the HS units and the C=O groups of the MIPOSS units.[45] Nevertheless, the values of T_g of the poly(AS-*alt*-MIPOSS) and poly(HS-*alt*-MIPOSS) alternating copolymers were significantly lower than those of PAS (T_g = 122 °C) and PHS (T_g = 150 °C) of similar molecular weights, and even lower than that of poly(S-*alt*-MIPOSS) lacking the AcO and OH functional groups. The glass transition temperature of PAS is higher than that of PS because the functional AcO groups of PAS enhances the intermolecular dipole–dipole interactions among the C=O groups of the PAS segments; after deacetylation to form PHS, the glass transition temperature would increase further because of intermolecular hydrogen bonding among the OH groups of the PHS segments. A possible reason for the low value of T_g of poly(AS-*alt*-MIPOSS) is that the self-association dipole-

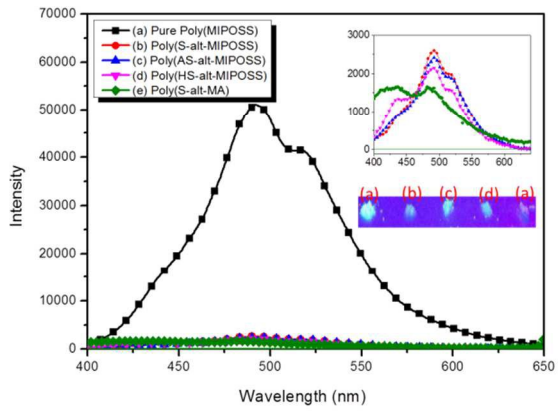

Figure 13: PL spectra of (a) poly(MIPOSS), (b) poly(S-*alt*-MIPOSS), (c) poly(AS-*alt*-MIPOSS), (d) poly(HS-*alt*-MIPOSS), and (e) poly(S-*alt*-MA) in solid state recorded with excitation at 330 nm. Photographs of poly(MIPOSS) and alternating copolymers in solid state under 365 nm UV illumination.

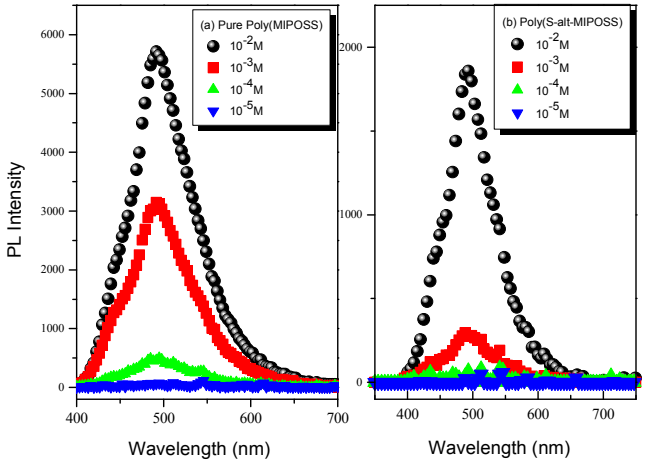

Figure 14: Fluorescence spectra of (a) poly(MIPOSS) and (b) poly(S-*alt*-MIPOSS) as solutions in THF at concentrations from 10^{-5} to 10^{-2} M (excitation at 330 nm).

dipole interactions of its AS···AS or MIPOSS···MIPOSS segments were disrupted significantly after inserting the AS units alternatively into the MIPOSS units. This hypothesis is consistent with the significant decrease in the widths at half-height, from 32.3 cm^{-1} for poly(MIPOSS) to 20.2 cm^{-1} for poly(AS-*alt*-MIPOSS), in the FTIR spectra. Scheme 1 and Figure 8 reveal that the alternative insertion of bulky MIPOSS units into PAS segments strongly hindered the self-association dipole-dipole interactions (inter- or intra-chain) among the PAS segments; thus, the bulky POSS units provided a strong screening effect that decreased the possibility of intermolecular interaction, thereby lowering the value of T_g. A similar reason might also explain the lower value of T_g of poly(HS-*alt*-MIPOSS): the inter- and intra-chain hydrogen bonding of the self-associating OH···OH groups of PHS would decrease significantly as a result of the strong intramolecular screening effect of bulky MIPOSS units. Such OH groups from the HS units would be able to interact only with the C=O groups of the MIPOSS units through weaker intra-chain OH···O=C hydrogen bonding. Therefore, the broad band at 3350 cm^{-1} representing strong self-association of the OH···OH units of PHS shifted to a higher wavenumber of 3453 cm^{-1} for the weaker inter-association of OH···O=C groups; correspondingly, the value of T_g decreased because no strong intermolecular hydrogen bonding interactions could occur among the PHS segments.

We recorded WAXD patterns (**Figure 11**) of poly(MIPOSS), poly(S-*alt*-MIPSS), poly(AS-*alt*-MIPOSS), and poly(HS-*alt*-MIPOSS) at room temperature to examine their crystallinity. The WAXD profile of poly(MIPOSS) features four major diffraction peaks at 7.06 (101), 9.50 (110), 10.60 (102), and 16.43 (113) corresponding to the rhombohedral crystal structure of MIPOSS;[49,50] accordingly, we observed a melting temperature, through DSC analyses, in Figure 10. After alternative insertion of S, AS, and HS inert diluent segments into the MIPOSS segment, the WAXD patterns of poly(S-*alt*-MIPSS), poly(AS-*alt*-MIPOSS), and poly(HS-*alt*-MIPOSS) featured only broad peaks, with the crystalline peaks of poly(MIPOSS) disappearing; thus, these alternating copolymers had amorphous structures, consistent with DSC analyses in **Figure 10**.

We performed TGA analyses under a N_2 atmosphere (**Figure 12**) to determine the decomposition temperatures (T_{d10} as standard) and char yields of these alternating copolymers prepared through free radical copolymerization. The degradation temperature and char yield of poly(MIPOSS) (345 °C and 14.8%, respectively) were higher than those of PS (337 °C and 0%, respectively), consistent with the readier pyrolysis of the PS main chain from 300 to 450 °C.[51,52] More interestingly, the value of T_{d10} and the char yield of poly(S-*alt*-MIPOSS) (397 °C and 9.5%, respectively) were higher than those of the standard PS as a result of the steric bulk of the rigid-cage MIPOSS units. In contrast, both the poly(AS-*alt*-MIPOSS) (376 °C and 28.1%, respectively) and poly(HS-*alt*-MIPOSS) (366 °C and 29.3%, respectively) alternating copolymers displayed relatively lower degradation temperatures and relatively higher char yields than those of poly(S-*alt*-MIPOSS) because, above their decomposition temperature, their acetyl and phenol moieties would tend to form aromatic char structures and increase the crosslinking densities of their organic/inorganic copolymers.[50a]

Optical Properties of Poly(MIPOSS), Poly(S-*alt*-MIPOSS), Poly(AS-*alt*-MIPOSS), and Poly(HS-*alt*-MIPOSS)

Poly(MIPOSS), poly(S-alt-MIPOSS), poly(AS-alt-MIPOSS), poly(HS-alt-MIPOSS) and poly(S-alt-MA) are soluble in THF, $CHCl_3$, DCM and DMF solution. The UV-Vis absorption spectrum of poly(MIPOSS) and others alternating copolymers in THF solution is shown in **Figure S2**. Poly(MIPOSS) and others alternating copolymers showed two major absorption peaks which can be assigned to the π-π* and n-π* transitions. The values of two major absorption peaks are summarized in **Table 1**.

We used PL spectroscopy to investigate the emission properties of the homopolymer and the alternating copolymers in the solid state and the fluorescence behavior of poly(MIPOSS) and poly(S-*alt*-MIPOSS) at various concentrations (from 10^{-5} to 10^{-2} M) in THF with excitation at 330 nm. **Figure 13** presents the PL spectra of poly(MIPOSS), poly(S-*alt*-MIPOSS), poly(AS-*alt*-MIPOSS), and poly(HS-*alt*-MIPOSS) in the solid state. The intensities of the unexpected emissions of the oxygenic nonconjugated poly(MIPOSS) at 490 and 519 nm were higher than those of the alternating copolymers, presumably because of the clustering of the locked C=O groups.[15,16] On the other hand, poly(S-*alt*-MIPOSS), poly(AS-*alt*-MIPOSS), and poly(HS-*alt*-MIPOSS) exhibited fluorescence that resulted from pi–pi interactions between the phenyl rings and C=O groups in poly(MIPOSS). In addition, the emission intensities of the copolymers were lower than those of poly(MIPOSS), suggesting a lower degree of clustering of the locked C=O units of

poly(MIPOSS) after alternative insertion of the styrene derivatives. **Figure S3** displays the photoluminescence spectra of poly(MIPOSS), poly(S-alt-MIPOSS), poly(AS-alt-MIPOSS), poly(HS-alt-MIPOSS) and poly(S-alt-MA) in THF solution (10^{-3} M). As shown in Figure S3, poly(MIPOSS) shows a strong emission peak at 496 nm, referring to its bulky anhydride group in maleimide isobutyl unit, which hinders the free rotation of polymer chains along C-C single bond.[16b] **Figure 14** displays the effect of concentration on the emission behavior of poly(MIPOSS) and poly(S-*alt*-MIPOSS) in THF. The emission intensities of both poly(MIPOSS) and poly(S-*alt*-MIPOSS) increased upon increasing the concentration (from 10^{-5} to 10^{-2} M) in THF. In the most dilute solutions (10^{-5} M) of these oxygenic nonconjugated polymers, we observed no emissions because only a small amount of the luminogen was present.[9c,12b,16,54] To examine the aggregation induced emission behavior of poly(MIPOSS) and poly(S-alt-MIPOSS), effect of water content on photoluminescence spectra were performed in THF/water mixture as predicted in **Figure S4**. Water is used here because it is a poor solvent for poly(MIPOSS) and poly(S-alt-MIPOSS), respectively. When an increasing water content from 0 to 80%, the corresponding solution in solution mixtures exhibited increase emission intensity due to aggregate of luminogenic molecules with high water contents. The formation of nanoaggregate structure has role to activate the restriction of intramolecular rotation (RIR) process. According to the concentration-enhanced emissions and solvent pair effect in **Figures 14(A)** and **14(B) and Figure S4**, we suspect that poly(MIPOSS) and poly(S-*alt*-MIPOSS) may both be AIE materials. To confirm our hypothesis, we measured the quantum efficiencies (Φ_f) of poly(MIPOSS), poly(S-*alt*-MIPOSS), poly(AS-*alt*-MIPOSS), poly(HS-*alt*-MIPOSS), and poly(S-*alt*-MA) in the solid state, obtaining values of 72.5, 55.5, 46.8, 7.0, and 6.9 %, respectively. Interestingly, the quantum efficiency of poly(S-*alt*-MIPOSS) was higher than that of poly(S-*alt*-MA), presumably because the POSS units were able to lock the C=O groups in the MIPOSS segments and, thereby, enhances the emission properties. In addition, the values of quantum efficiencies (Φ_f) of poly(MIPOSS), poly(S-alt-MIPOSS), poly(AS-alt-MIPOSS), poly(HS-alt-MIPOSS), and poly(S-alt-MA) in THF solution were 57.82, 5.52, 2.70, 5.64 and 1.72%, respectively. Dynamic light scattering (DLS) was measured to determine poly(MIPOSS) and poly(S-alt-MIPOSS) can form nanoaggregates structure in THF/H_2O mixture solution as provided in **Figure S5**. The sizes of particles of poly(MIPOSS) were 733, 580, 383, 225 nm. While, the sizes of particles of poly(S-alt-MIPOSS) were 906, 774, 728 and 586 nm when increasing water content from 40 to 80% in the THF/water mixture media. The formation of shrunken aggregates of poly(MIPOSS) and poly(S-alt-MIPOSS) in solution with increasing water volume fraction are responsible for the emission intensity enhancement in **Figure S4.**

Conclusions

We have synthesized a poly(MIPOSS) homopolymer and poly(S-*alt*-MIPOSS), poly(AS-*alt*-MIPOSS), and poly(HS-*alt*-MIPOSS) alternating copolymers through facile free radical polymerizations, and characterized their chemical structures using NMR spectroscopy, FTIR spectroscopy, and MALDI-TOF mass spectrometry. TGA revealed that the thermal degradation temperatures and char yields of the POSS-containing alternating copolymers were improved after incorporation of the MIPOSS units. Interestingly, WXRD analysis indicated that poly(MIPOSS) was a crystalline polymer, whereas the POSS-containing alternating polymers, formed after alternating insertion of styrene derivatives, were amorphous polymers. In addition, the emission of the oxygenic nonconjugated poly(MIPOSS) was stronger in the bulk state and its quantum efficiency was higher than those of the POSS-containing alternating copolymers; the emission of poly(MIPOSS) was associated with the molecular interactions between the five-membered dihydrofuran-2,5-dione rings and its highly crystallinity, as determined using PL spectroscopy and WXRD. A further study of the fluorescence mechanism of these POSS-containing alternating polymers might lead to the design of novel luminescent polymeric materials with various potential applications.

Acknowledgment

This study was supported financially by the Ministry of Science and Technology, Taiwan, Republic of China, under contracts MOST103-2221-E-110-079-MY3 and MOST102-2221-E-110-008-MY3.

References

1. (a) W. Zhang, L. Xu, J. Qin and C. Yang, *Macromol. Rapid Commun.*, 2013, **34**, 442-446. (b) D. D. Li, J. H. Yu and R. R. Xu, *Chem. Commun.*, 2011, **47**, 11077-11079. (c) Z. Song, Y. Hong, R. T. K. Kwok, J. W. Y. Lam, B. Liu and B. Z. Tang, *J. Mater. Chem. B*, 2014, **2**, 1717-1723.
2. (a) L. Prodi, F. Bolletta, M. Montali and N. Zaccheroni, *Coord. Chem. Rev.*, 2000, **205**, 59-83. (b) B. Wang and M. R. Wasielewski, *J. Am. Chem. Soc.*, 1997, **119**, 12-21.
3. K. Dore, S. Dubus, H. A. Ho, I. Levesque, M. Bruntte, G. Corbeil, M. Boissinot, G. Boivin, M. G. Bergeron, D. Boudreau and M. Leclerc, *J. Am. Chem. Soc.*, 2004, **126**, 4240-4244.
4. A. Keppler, H. Pick, C. Arrivoli, H. Vogel and K. Johnsson, *Proc. Natl. Acad. Sci. U. S. A.*, 2004, **101**, 9955-9959.
5. (a) D. D. Li, C. L. Miao, X. D. Wang, X. H. Yu, J. H. Yu and R. R. Xu, *Chem. Commun.*, 2013, **49**, 9549-9551. (b) Y. X. Wu, J. B. Li, L. H. Liang, D. Q. Lu, L. Zhang, G. J. Mao, L. Y. Zhou, X. B. Zhang, W. Tan, G. L. Shen and R. Q. Yu, *Chem. Commun.*, 2014, **50**, 2040-2042.
6. (a) Y. Song, S. Zhu and B. Yang, *RSC Adv.*, 2014, **4**, 27184-272000. (b) A. P. Alivistos, *Science*, 1996, **271**, 933-937.
7. M. Li, L. H. Feng, H. Y. Lu, S. Wang and C. F. Chen, *Adv. Funct. Mater.*, 2014, **24**, 4405-4412.
8. (a) D. C. Chudakov, M. V. Matz, S. Lukyanov and K. A. Lukyanov, *Physiol Rev.*, 2010, **90**, 1103-1163. (b) J. N. Brantely, C. B. Bailey, J. R. Cannon, K. A. Clark, D. A. V. Bout, J. S. Brodbelt, A, T. K. Clay and C. W. Bielawski, *Angew. Chem. Int. Ed.*, 2014, **53**, 5088-5092.
9. (a) J. H. Wu and G. S. Liou, *Polym. Chem.*, 2015, **6**, 5225-5232. (b) B. P. Jiang, D. S. Guo, Y. C. Liu, K. P. Wang and Y. Liu, *ACS Nano*, 2014, **8**, 1609-1618. (c) L. Liu, B. Wu, P. Yu, R. X. Zhuo and S. W. Huang, *Polym. Chem.*, 2015, **6**, 5185-5189. (d) S. H. Huang, Y. W. Chaing, J. L. Hong, *Polym. Chem.*, 2015, **6**, 497-508.
10. (a) C. Munkholm, D. R. Parkinson and D. R. Walt, *J. Am. Chem. Soc.*, 1990, **112**, 2608-2612. (b) W. Dong, T. Fei, A. P. Cando and U. Scherf, *Polym. Chem.*, 2014, **5**, 4048-4053.
11. (a) M. Belletete, J. Bouchard, M. Leclerc and G. Durocher, *Macromolecules*, 2005, **38**, 880-887. (b) R. Jakubiak, C. J. Collison, W. C. Wan and L. Rothberg, *J. Phys. Chem. A*, 1999, **103**, 2394-2401.
12. (a) A. Qin, J. W. Y. Lam, B. Z. Tang, *Prog. Polym. Sci.*, 2012, **37**, 182-209. (b) Y. Gong, L. Zhao, Q. Peng, D. Fan, W. Z. Yuan, Y. Zhang and B. Z. Tang, *Chem. Sci.*, 2015, **6**, 4438-4444.
13. (a) L. Li, M. Chen, H. Zhang, H. Nie, J. Z. Sun, A. Qin and

B. Z. Tang, *Chem. Commun*., 2015, **51**, 4830-4833. (b) Y. Hong, J. W. Y. Lam and B. Z. Tang, *Chem. Soc. Rev*., 2011, **40**, 5361-5388. (c) S. Bao, Q. Wu, W. Qin, Q. Yu, J. Wang, G. Liang and B. Z. Tang, *Polym. Chem*., 2015, **6**, 3537-3542.

14. (a) X. Lou, Z. Zhao, Y. Hong, C. Dong, X. Min, Y. Zhuang, X. Xu, Y. Jia, F. Xia and B. Z. Tang, *Nanoscale*, 2014, **6**, 14691-14696. (b) N. Zhao, M. Li, Y. Yan, J. W. Y. Lam, Y. L. Zhang, Y. S. Zhao, K. S. Wong and B. Z. Tang, *J. Mater. Chem. C*, 2013, **1**, 4640-4646. (c) J. Chen, Z. Xie, J. W. Y. Lam, C. C. W. Law and B. Z. Tang, *Macromolecules*, 2003, **36**, 1108-1117. (d) J. Chen, C. C. W. Law, J. W. Y. Lam, Y. Dong, S. M. F. Lo, I. D. Williams, D. Zhu and B. Z. Tang, *Chem. Mater*., 2003, **15**, 1535-1546.
15. T. Huang, Z. Wang, A. Qin, J. Z. Sun and B. Z. Tang, *Acta Chim. Sinica*., 2013, **71**,973- 979.
16. (a) E. Zhao, J. W. Y. Lam, L. Meng, Y. Hong, H. Deng, G. Bai, X. Huang, J. Hao and B. Z. Tang, *Macromolecules*, 2015, **48**, 64-71. (b) W. C. Kim and D. C. Lee, *Polym. Eng. Sci*., 1995, **35**, 1600-1604.
17. R. B. Restani, P. I. Morgado, M. P. Ribeiro, I. J. Correia, A. A. Ricardo and V. D. B. Bonifacio, *Angew. Chem. Int. Ed*., 2012, **51**, 5162-5165.
18. Y. Lin, J. W. Gao, H. W. Liu and Y. S. Li, *Macromolecules*, 2009, **42**, 3237-3246.
19. (a) D. Wang, Z. Q. Yu, C. Y. Hong and Y. Z. You, *Eur. Polym. J*., 2013, **49**, 4189-4197. (b) Y. Z. You, Z. Q. Yu, M. M. Cui and C. Y. Hong, *Angew. Chem. Int. Ed*., 2010, **49**, 1099-1102.
20. M. Sun, C. Y. Hong and C. Y. Pan, *J. Am. Chem. Soc*., 2012, **134**, 20581-19584.
21. Y. Liu and H. S. Goh, *Macromolecules*, 2005, **38**, 9906-9909.
22. D. Wang and T. Imae, *J. Am. Chem. Soc*., 2004, **126**, 13204-13205.
23. M. R. Eftink, T. J. Selva and Z. Wasylewski, *Photochem. Photobiol*., 1987, **46**, 23-30.
24. A. Pucci, R. Rausa and F. Ciaredlli, *Macromol. Chem. Phys*., 2008, **209**, 900-906.
25. C. C. Wang, Z. X. Guo, S. K. Fu, W. Wu and D. B. Zhu, *Prog. Polym. Sci*., 2004, **29**, 1079-1141.
26. S. W. Kuo and F. C. Chang, *Prog. Polym. Sci*., 2011, **36**, 1649-1696.
27. A. Fina, O. Monticelli and G. Gamino, *J. Mater. Chem*., 2010, **20**, 9297-9305.
28. K. W. Huang, L. W. Tsai and S. W. Kuo, *Polymer*, 2009, **50**, 4876-4887.
29. (a) Y. Li, H. Su, X. Feng, Z. Wang, K. Guo, C. Wesdemioitis, Q. Fu, S. Z. D. Cheng and W. B. Zhang, *Polym. Chem*., 2014, **5**, 6151-6162. (b) M. Huang, C. H. Hsu, J. Wang, S. Mei, X. Dong, Y. Li, M. Li, H. Liu, W. Zhang, T. Aida, W. B. Zhang, K. Yue, and S. Z. D. Cheng, *Science*, 2015, **348**, 424-428. (c) Y. Li, H. Su, X. Fneg, K. Yue, Z. Wang, Z. Lin, X. Zhu, Q. Fu, Z. B. Zhang, S. Z. D. Cheng, and W. B. Zhang, *Polym. Chem.,* 2015, **6**, 827-837.
30. C. F. Huang, S. W. Kuo, F. J. Lin, W. J. Huang, C. F. Wang, W. Y. Chen and F. C. Chang, *Macromolecules*, 2006, **39**, 300-308.
31. R. Y. Kannan, H. J. Salacinski, P. E. Butler and A. M. Seifalian, *Acc. Chem. Res*., 2005, **38**, 879-884.
32. D. B. Cordes, P. D. Lickiss and F. Rataboul, *Chem. Rev*., 2010, **110**, 2081-2173.
33. M. D. Disney, J. Zheng, T. M. Swager and P. H. Seeberger, *J. Am. Chem. Soc*., 2004, **126**, 13343-13346.
34. B. A. Griffin, S. R. Adams and R. Y. Tsien, *Science*, 1998, **281**, 269-272.
35. J. Wu and P. T. Mather, *Polym. Rev*., 2009, **49**, 25-63.
36. Y. Tada, H. Yoshida, Y. Ishida, T. Hirai, J. K. Bosworth, E. Dobisz, R. Ruiz, M. Takenaka, T. Hayakawa and H. Hasegawa, *Macromolecules*, 2012, **45**, 9347-9356.
37. T. Hirai, M. Leolukman, T. Hayakawa, M. Kakimoto and P. Gopalan, *Macromolecules*, 2008, **41**, 4558-4560.
38. Y. Ishida, T. Hirai, R. Goseki, M. Tokita, M. A. Kakimoto and T. Hayakawa, *J. Polym. Sci., Part A: Polym. Chem*., 2011, **49**, 2653-2664.
39. E. S. Cozza, V. Bruzzo, F. Carniato, E. Marsano and O. Monticelli, *ACS. Appl. Mater. Interfaces*, 2012, **4**, 604-607.
40. Z. Zhang, L. Hong, Y. Gao and W. Zhang, *Polym. Chem*., 2014, **5**, 4534-4541.
41. Z. Zhang, L. Hong, J. Li, F. Liu, H. Cai, Y. Gao and W. Zhang, *RSC Adv*., 2015, **5**, 21580-21587.
42. (a) Y. Syuan and S. W. Kuo, *RSC Adv*., 2014, **4**, 34849-34859. (b) Y. J. Yen, S. W. Kuo, C. F. Huang, J. K. Chen and F. C. Chang, *J. Phys. Chem. B*, 2008, 112, 10821-10829. (c) S. W. Kuo, H. C. Lin, W. J. Huang, C. F. Huang and F. C. Chang, *J. Polym. Sci., Part B: Polym. Phys*., 2006, **44**, 673-686.
43. Y. H. Zhang, J. Huang and Y. M. Chen, *Macromolecules*, 2005, **38**, 5069-5077.
44. J. Z. Du and Y. M. Chen, *Macromolecules*, 2004, **37**, 6322-6328.
45. S. W. Kuo and C. J. Chen, *Macromolecules*, 2012, **45**, 2442-2452.
46. P. O. Danis and E. D. Karr, Org. *Mass Spectrom.*, 1993, 28, 923-925.
47. L. R. Hutchings, P. P. Brooks, D. Parker, J. A. Mosely and S. Sevinc, *Macromolecules*, 2015, **48**, 610-628.
48. D. C. Schriemer, L. Li, *Anal. Chem*., 1996, **68**, 2721-2725.
49. (a) L. Cui, J. P. Collet, G. Xu, L. Zhu, *Chem. Mater*., 2006, **18**, 3503-3512. (b) Y. J. Sheng, W. J. Lin and W. C. Chen, *J. Chem. Phys*., 2004, **121**, 9693-9701.
50. (a) Y. C. Sheen, C. H. Lu, C. F. Huang, S. W. Kuo and F. C. Chang, *Polymer*., 2008, **49**, 4017-4024. (b) A. J. Waddon and E. B. Coughlin, *Chem. Mater*., 2003,**15**, 4555-4561.
51. R. Ding, Y. Hu, Z. Gui, R. Zong, Z. Chen and W. Fan, *Polym. Degrad. Stab*., 2003, **81**, 473-476.
52. M. Suzuki and C. A. Wilkie, *Polym. Degrad. Stab*., 1995, **47**, 217-221.
53. J. J. Yan, Z. K. Wang, X. S. Lin, C. Y. Hong, H. J. Liang, C. Y. Pan and Y. Z. You, *Adv. Mater*., 2012, **24**, 5617-5624.
54. G. M. Mohamed, H. F. Lu, J. L. Hong, S. W. Kuo, *Polym. Chem*., 2015, **8,** 6340-6350.

Graphic Abstract

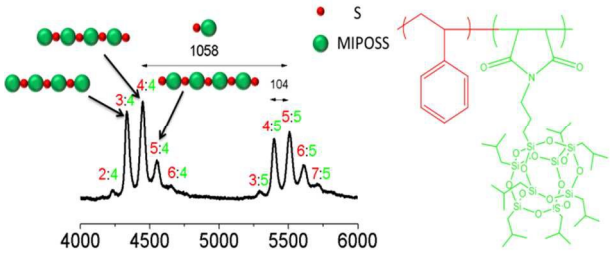

Unusual fluorescent polyhedral oligomeric silsesquioxane (POSS)-containing polymers lacking any common fluorescent units because of the crystallinity and clustering of locked C=O groups of POSS units.